

## Arbitrarily-shaped microgels composed of chemically unmodified biopolymers

Vakkipurath Kodakkadan, Yadu N.; Idzakovicova, Kristyna; Sepitka, Josef; Ten Napel, Daniël; Safai, Eric; Cigler, Petr; Štěpánek, Frantisek; Rehor, Ivan

**DOI**

[10.1039/c9bm02056j](https://doi.org/10.1039/c9bm02056j)

**Publication date**

2020

**Document Version**

Final published version

**Published in**

Biomaterials Science

**Citation (APA)**

Vakkipurath Kodakkadan, Y. N., Idzakovicova, K., Sepitka, J., Ten Napel, D., Safai, E., Cigler, P., Štěpánek, F., & Rehor, I. (2020). Arbitrarily-shaped microgels composed of chemically unmodified biopolymers. *Biomaterials Science*, 8(11), 3044-3051. <https://doi.org/10.1039/c9bm02056j>

**Important note**

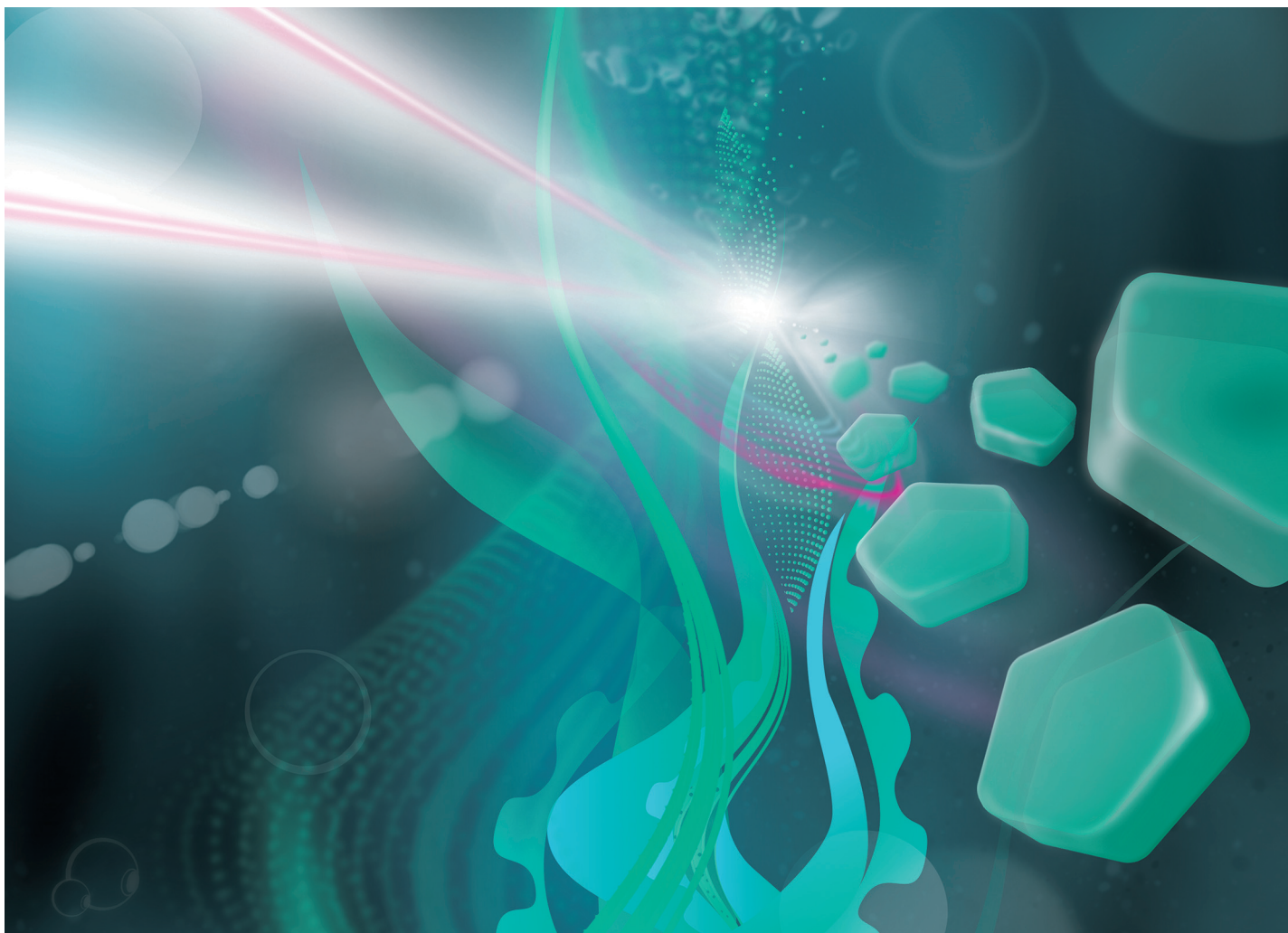
To cite this publication, please use the final published version (if applicable).  
Please check the document version above.

**Copyright**

Other than for strictly personal use, it is not permitted to download, forward or distribute the text or part of it, without the consent of the author(s) and/or copyright holder(s), unless the work is under an open content license such as Creative Commons.

**Takedown policy**

Please contact us and provide details if you believe this document breaches copyrights.  
We will remove access to the work immediately and investigate your claim.



**Highlighting a research article from the Hydrogel Machines group at University of Chemistry and Technology, Prague, Czech Republic.**

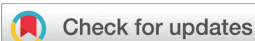
Arbitrarily-shaped microgels composed of chemically unmodified biopolymers

This article introduces a method for the production of microgels of any desired shapes, composed purely from chemically unmodified biopolymers, such as alginate obtained from seaweed. Although such biopolymers are not photosensitive, the desired shape of the microgel is obtained *via* a photochemical process.

**As featured in:**



See Ivan Rehor *et al.*, *Biomater. Sci.*, 2020, **8**, 3044.



Cite this: *Biomater. Sci.*, 2020, **8**, 3044

## Arbitrarily-shaped microgels composed of chemically unmodified biopolymers†

Yadu N. Vakkipurath Kodakkadan,<sup>a</sup> Kristyna Idzakovicova,<sup>a</sup> Josef Sepitka,<sup>b</sup> Daniël ten Napel,<sup>c</sup> Eric Safai,<sup>d</sup> Petr Cigler,<sup>e</sup> Frantisek Štěpánek<sup>a</sup> and Ivan Rehor<sup>b</sup> \*<sup>a,e</sup>

Biohydrogels, composed of naturally occurring biopolymers are typically preferred over their synthetic analogues in bioapplications thanks to their biocompatibility, bioactivity, mechanical or degradation properties. Shaping biohydrogels on the single-cell length scales (micrometers) is a key ability needed to create bioequivalent artificial cell/tissue constructs and cannot be achieved with current methods. This work introduces a method for photolithographic synthesis of arbitrarily shaped microgels composed purely of a biopolymer of choice. The biopolymer is mixed with a sacrificial photocrosslinkable polymer, and the mixture is photocrosslinked in a lithographic process, yielding anisotropic microgels with the biopolymer entrapped in the network. Subsequent ionic or covalent biopolymer crosslinking followed by template cleavage yields a microgel composed purely of a biopolymer with the 3D shape dictated by the photocrosslinking process. Method feasibility is demonstrated with two model polysaccharide biopolymers (alginate, chitosan) using suitable crosslinking methods. Next, alginate microgels were used as microtaggants on a pharmaceutical oral solid dose formulation to prevent its counterfeiting. Since the alginate is approved as an additive in the food and pharmaceutical industries, the presented tagging system can be implemented in practical use much easier than systems comprising synthetic polymers.

Received 21st December 2019,  
Accepted 12th April 2020

DOI: 10.1039/c9bm02056j

rs.c.li/biomaterials-science

## Introduction

Hydrogel materials are widely used in bioapplications. The ability to precisely define the hydrogel shape is often essential for its desired function in a biological environment. Shaping hydrogels with micrometre precision *i.e.* on the level of single cells, has enabled their application as artificial cells,<sup>1,2</sup> drug<sup>3</sup> or cell<sup>4</sup> delivery carriers, and elemental units assembled in artificial tissue constructs.<sup>5,6</sup> Shaping microgels at these length scales is not accessible by bioprinting methods and requires lithographic methods,<sup>7</sup> as was recently demonstrated with photolithography,<sup>8</sup> imprint lithography (PRINT)<sup>9</sup> and

stop-flow lithography (SFL).<sup>10–12</sup> These lithographic methods require synthetic photocrosslinkable polymers as hydrogel precursors.<sup>7</sup> Photocrosslinkability has been achieved by attaching a (meth)acrylate moiety to a polymer of choice, such as polyethylene glycol (PEG),<sup>1,13,14</sup> block copolymers of polyesters and PEG,<sup>15</sup> polysaccharides,<sup>16,17</sup> and proteins.<sup>18</sup>

Although acrylated polymers are widely used in biomedical research *in vitro*, they can exhibit undesired interactions with living systems after *in vivo* application, resulting in harmful effects.<sup>19</sup> Immune response to acrylates, methacrylates and their polymerization products has been widely reported<sup>20–23</sup> (*e.g.* well described allergy to polyHEMA in contact lenses<sup>24</sup>). The prevalence of such intolerances is on the rise due to the omnipresence of acrylate-based materials.<sup>25</sup> Avoiding such materials is hence highly desired in biomedical applications, where close contact between the material and a living system is required. Biopolymers (*i.e.* polymers produced by living organisms) are typically well-tolerated in living systems and are therefore generally preferred over synthetic polymers for bioapplications.<sup>19,26–29</sup> Moreover, the potential bioactivity of a biopolymer can lead to a truly biomimetic interface. The naturally occurring crosslinking mechanisms of biopolymers vary, but none are directly triggered by light. Methacrylation, which is required for photolithographic processing of biopolymers, represents an extra synthetic step and, furthermore, it can negatively affect their tolerability, bioactivity or metaboli-

<sup>a</sup>University of Chemistry and Technology, Department of Chemical Engineering, Technická 5, 16628 Prague, Czech Republic. E-mail: rehori@vscht.cz

<sup>b</sup>Czech Technical University in Prague, Faculty of Mechanical Engineering, Department of Mechanics, Biomechanics and Mechatronics, Technická 4, 160 00 Prague, Czech Republic

<sup>c</sup>Utrecht University, Van 't Hoff Laboratory for Physical and Colloid Chemistry, Debye Institute for Nanomaterials, Padualaan 8, 3584 Utrecht, The Netherlands

<sup>d</sup>Delft University of Technology, Process & Energy Department, Faculty of Mechanical Engineering, Maritime and Material Science, Leeghwaterstraat 39, 2628CB Delft, The Netherlands

<sup>e</sup>Institute of Organic Chemistry and Biochemistry of the CAS, Flemingovo náměstí 2, 16000 Prague 6, Czech Republic

† Electronic supplementary information (ESI) available. See DOI: 10.1039/c9bm02056j

zation *in vivo*. To overcome this hurdle, significant effort has been devoted to shape the chemically non-modified (*i.e.*, pure) biopolymers. Current methods use either moulds<sup>30–34</sup> or indirect gelation methods in which a light-triggered reaction initiates the release of a gelation agent.<sup>35–38</sup> None of these methods, however, provides micron-scale resolution, that is a key step in the design of biocompatible materials with controlled interactions with real tissue organized on a cellular (*i.e.*, micron) level.<sup>1–4</sup>

In this work, we introduce a method for photolithographic synthesis of anisotropic microgels composed purely of a biopolymer of choice. The method uses a photocrosslinkable and degradable polymer as a sacrificial template. This polymer is lithographically processed in a mixture with the biopolymer to provide anisotropic hydrogels with the biopolymer physically entrapped, but not chemically bound, within their network. Subsequent crosslinking of the biopolymer followed by hydrolysis of the template yields anisotropic hydrogels composed solely of the biopolymer. We demonstrate the feasibility of this method with two model polysaccharide biopolymers using suitable crosslinking methods. Alginate is ionically crosslinked by divalent cations and chitosan is covalently crosslinked using genipin, a biocompatible crosslinker widely used for gelation of aminated polysaccharides or proteins in various bioapplications.<sup>39–41</sup> As a model lithographic method, we use stop-flow lithography, a microfluidic continuous lithographic method, capable of high throughput production of arbitrarily shaped hydrogel microparticles (microgels) from methacrylated polymers.<sup>10,15</sup> Furthermore, we demonstrate the practical application of prepared microgels as authenticity microtaggants for pharmaceutical products.

## Experimental section

### Materials

Dex-HEMA was synthesized and characterized as previously described,<sup>42</sup> dextran of  $M_r$  15–25 kDa (from *Leuc. spp.*, Sigma Aldrich) was used as a substrate and was modified to degrees of substitution (DS) of 20 and 25 molar percent methacrylate units per one sugar unit. The photoinitiator lithium phenyl-2,4,6-trimethylbenzoylphosphinate (LAP) was synthesized according to previously published procedures.<sup>43</sup>

### Dex-HEMA + alginate: pregel composition

A 15 mg portion of Dex-HEMA (15 kDa, 20% DS) was dissolved in 80  $\mu\text{L}$  of 2.5% (w/w) alginate. LAP solution (5  $\mu\text{L}$ , 0.25% w/v in water, 43 nmol) was added, and then fluorescein *o*-methacrylate (2  $\mu\text{L}$  of a 0.4% w/v solution in DMSO, 16 nmol) was added. The mixture was vortexed, sonicated, centrifuged (5 min at 13 000g) and used within several hours of preparation.

### Dex-HEMA + chitosan: pregel composition

A 15 mg portion of Dex-HEMA (15 kDa, 25% DS) was dissolved in 80  $\mu\text{L}$  of 3% (w/v) chitosan. LAP solution (5  $\mu\text{L}$ , 0.25% w/v in

water, 43 nmol) was added, and then methacryloxyethyl thio-carbamoyl rhodamine B (2  $\mu\text{L}$  of a 0.4% w/v solution in DMSO, 16 nmol) was added. The mixture was vortexed, sonicated, centrifuged (5 min at 13 000g) and used within several hours of preparation.

### SFL production

Manufacture of the microfluidic chips and the SFL process were performed as previously described,<sup>16</sup> with some adaptations. A 10 $\times$  objective was used for mask projection (instead of the previously used 40 $\times$ ) to reduce microgel sticking. The SFL process was controlled by an Arduino board, namely the synchronization of the consecutive steps (purge, irradiation) and changes in the irradiation positions between consecutive irradiations (typically, six positions were cycled in a loop followed by one purge). The production rate was around 10 000 particles per hour. Details can be found in the ESI.†

### Post-lithographic treatment of alginate Dex-HEMA microgels

After synthesis, the particles were collected and washed 5 times with water (diluted to 340  $\mu\text{L}$  and concentrated to 40  $\mu\text{L}$ ). Then,  $\text{CaCl}_2$  solution (2% w/v, 200  $\mu\text{L}$  per well) was added. This step was performed no later than 15 min after microgel collection; otherwise, a substantial fraction of the biopolymer leaked from the network, which resulted in compromised feature resolution or even complete collapse of the microgels after template removal. The neutral  $\text{CaCl}_2$  solution was replaced after 2 min with basic  $\text{CaCl}_2$  solution (10, 20 and 30 mM), freshly prepared under an inert atmosphere by rapidly adding 1 M NaOH (100  $\mu\text{L}$ , 200  $\mu\text{L}$  and 300  $\mu\text{L}$ , respectively) into  $\text{CaCl}_2$  (2% w/v, 10 mL) and filtering the precipitate through a 0.2  $\mu\text{m}$  syringe filter. During this step, the well plate was held under an inert atmosphere to avoid the formation of calcium carbonate precipitate. After 10 min, the particles were washed 3 times with 2%  $\text{CaCl}_2$  (diluted to 340  $\mu\text{L}$  and concentrated to 40  $\mu\text{L}$ ).

### Post-lithographic treatment of chitosan-Dex-HEMA microgels

After synthesis, the particles were collected and washed 3 times with water (diluted to 340  $\mu\text{L}$  and concentrated to 40  $\mu\text{L}$ ). The genipin solution was added (300  $\mu\text{L}$ , 10 mM in water, pH adjusted to 6.5). The sample was incubated for 2 h at 37  $^\circ\text{C}$  in the dark. The genipin solution was then replaced with a fresh one, followed by another 2 h of incubation. The crosslinked particles were washed 3 times with water (diluted to 340  $\mu\text{L}$  and concentrated to 40  $\mu\text{L}$ ). Particles were incubated with 1 M NaOH (300  $\mu\text{L}$ ) for 3 min, followed by incubation in water (10 min) and again in 1 M NaOH (300  $\mu\text{L}$ , 3 min). Finally, the sample was washed 5 times with water (diluted to 340  $\mu\text{L}$  and concentrated to 40  $\mu\text{L}$ ).

## Results and discussion

We exploit hydrolytic lability<sup>44</sup> of Dex-HEMA and used it as a template that can be rapidly decomposed on-demand. First,

we prepared a single-phase mixture comprising the template polymer Dex-HEMA, a biopolymer of choice (alginate or chitosan), and a water-soluble photoinitiator.<sup>43</sup> We synthesized microgels from this blend using SFL according to the scheme outlined in Fig. 1. A microfluidic channel was filled with the mixture, and microgels were created by local photocrosslinking of Dex-HEMA, their shape being defined by the photomask<sup>16</sup> (details of the mixture composition and process optimization can be found in the ESI†).

The synthesized microgels (Fig. 2A–C – alginate loaded microgels, microgel length =  $210 \pm 4 \mu\text{m}$ , Fig. 3A–C – chitosan loaded microgels, microgel length  $240 \pm 8 \mu\text{m}$ ) form semi-interpenetrated network (semi-IPN) – the crosslinked Dex-HEMA network preserves the shape defined in the lithographic process while the biopolymer is physically entrapped in this network. Both Dex-HEMA and the biopolymer are labelled with fluorescent dyes to keep track of the microgel composition during post-synthetic processing. In the next step, the entrapped biopolymer (alginate or chitosan) is crosslinked *via* a suitable method dictated by the nature of the biopolymer.

**Alginate** crosslinking and formation of interpenetrated network (IPN) was induced by exposing alginate-loaded Dex-HEMA microgels to calcium ions, which resulted in isotropic shrinkage of the microgels to a length of  $181 \pm 3 \mu\text{m}$  (14% reduction) (Fig. 2D–F). This shrinkage can be explained by the formation of new crosslinks, which reduces the hydrogel mesh size.<sup>45</sup> The IPN microgels showed no signs of composition non-uniformity on micron level, that would indicate phase separation of the two polymers, that may occur during the semi-IPN-

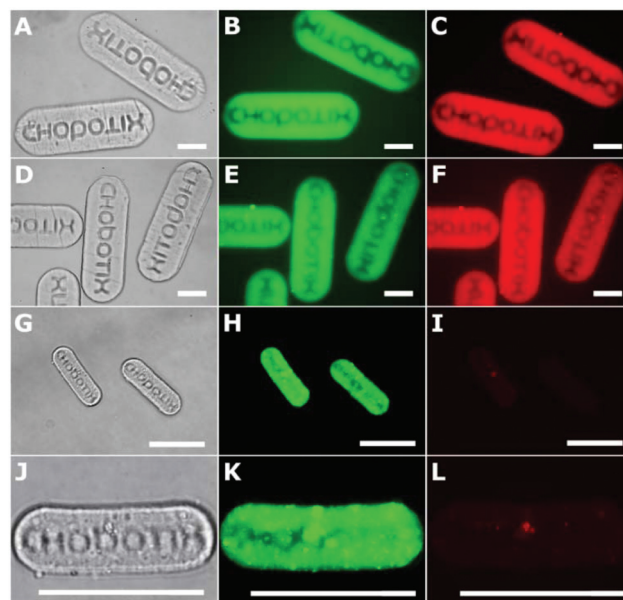


**Fig. 2** Micrographs of alginate anisotropic hydrogels. (A) Hydrogels obtained from lithographic synthesis consist of alginate physically entrapped in the structure of photocrosslinked Dex-HEMA. (B and C) Fluorescent images of labelled alginate and labeled Dex-HEMA network, respectively. (D–F) The same sample after the addition of  $\text{CaCl}_2$ . Panels show brightfield, alginate fluorescence, and Dex-HEMA fluorescence, respectively. (G–L) Samples after the addition of a base (brightfield – G and J; alginate fluorescence – H and K; Dex-HEMA fluorescence – I and L). Scale bars correspond to  $50 \mu\text{m}$ . All fluorescence images are in false color.

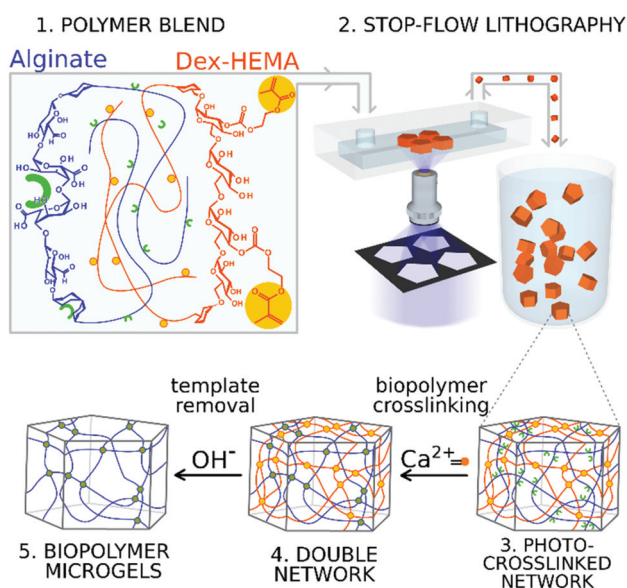


**Fig. 1** Scheme of anisotropic bio-microgel synthesis. A mixture of the photocrosslinkable degradable polymer Dex-HEMA and a biopolymer (alginate is shown as an example) is processed *via* stop-flow lithography. The resulting microgels are treated with calcium ions to crosslink alginate entrapped in the Dex-HEMA hydrogel matrix. In the last step, the template matrix of Dex-HEMA is basically hydrolyzed and washed away, yielding pure alginate particles.

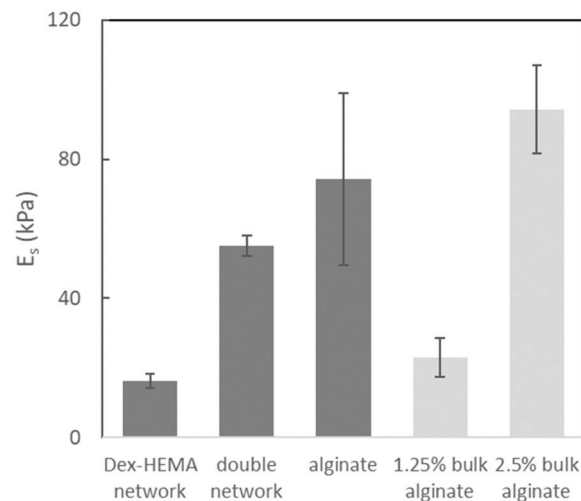


**Fig. 3** Elastic modulus of alginate microgels during postprocessing. From left: fresh microgels as produced by lithographic process, cross-linked by Dex-HEMA; double network Dex-HEMA, alginate microgels; alginate microgels after the Dex-HEMA cleavage; bulk hydrogel prepared from 1.25% sodium alginate solution; bulk hydrogel prepared from 2.5% sodium alginate solution.

IPN transition (Fig. S1†). A similar IPN comprising Dex-HEMA and alginate has been previously prepared (in reversed cross-linking order) in bulk and studied as an injectable scaffold.<sup>46,47</sup>

In the next step, we exposed the IPN anisotropic microgels to a basic solution to accelerate the hydrolysis of the Dex-HEMA network.<sup>42,44</sup> The basic solution contained  $\text{Ca}^{2+}$  ions to stabilize the alginate hydrogel during Dex-HEMA hydrolysis; in the absence of  $\text{Ca}^{2+}$ , the microgels fully dissolved. Hydrolysis took several minutes, with a loss in fluorescence signal from the Dex-HEMA network marking its completion (Fig. 2I and L). The hydrolysis rate (controlled by the hydroxide concentration) determined the size and shape fidelity of the resulting microgels. Faster hydrolysis produced smaller particles with a higher fidelity of the features and the best results were achieved when hydrolysis took no more than 3 minutes (30 mM NaOH). In this case, the particles shrunk to a length of  $52 \pm 2 \mu\text{m}$ , which corresponds to 71% shrinkage in linear dimensions compared to the IPN microgels (Fig. 2G–L). This corresponds to a 97.5% volume loss in this step, while, remarkably, the microgel shape and size uniformity is preserved. Highly fluorescent agglomerates are visible within the alginate microgels (Fig. 2J and K). We also observed such agglomerates in our alginate stock solutions. Their frequency can be reduced by filtration of the diluted alginate stock solution through a  $0.2 \mu\text{m}$  filter, but they reappear over the course of long-term storage (within days).

A lower sodium hydroxide concentration (20 mM) led to slower Dex-HEMA hydrolysis ( $\sim 10$  min) resulting in lower shrinkage ratios (by  $\sim 50\%$ ). This process provided microgels with well-resolved outside shape, but small details (such as the text 'CHOBOTIX') were not clear (Fig. S2†). Such conditions can be used for the preparation of anisotropic hydrogels with simple shapes, such as pentagonal prisms (Fig. S3,† the kinetics of the hydrolysis process are shown in Fig. S4†). Even slower hydrolysis rates (10 mM NaOH) produced microgels with blurred or completely unresolved features. Interestingly, we obtained well-resolved alginate hydrogels when alginate crosslinking and template hydrolysis were merged into a single step by adding the basic  $\text{CaCl}_2$  solution directly to the freshly SFL-produced microgels (Fig. S5†). This demonstrates that the rate of calcium crosslinking is faster than the rate of Dex-HEMA hydrolysis. The underlying phenomena, currently investigated by both theory and simulation approach, are beyond the scope of this work and the results will be reported elsewhere. Generally speaking, hydrogel volume shrinkage during cross-linking is a complex interplay of various phenomena like cross-link formation, water diffusion, hydrogen bonding between water molecules and hydrophilic polymer chains, and others.<sup>48</sup> Dynamics of the cross-linking process can be predicted using molecular dynamics (MD) and coarse-grained (mesoscale) dissipative particle dynamics (DPD),<sup>49,50</sup> or continuum mechanics models based on reaction–diffusion equations.<sup>51</sup> The thermodynamics of polymer–solvent and polymer–polymer interactions is typically treated *via* Flory–Huggins theory<sup>52</sup> with the inter-species interaction parameters estimated using Hansen solubility theory,<sup>53</sup> which assumes contribution of three inter-atomic forces (dispersion force, polar force and hydrogen bonding).

Alternatively, we employed dextranase for enzymatic cleavage<sup>54</sup> of Dex-HEMA to avoid exposure to harsh basic conditions during microgel synthesis and to open the door for future opportunities to load sensitive cargo into microgels. The enzymatic cleavage took 2 h and resulted in shrinkage of the microgel by 41% in linear dimensions compared to the IPN microgels, while simultaneously providing good shape fidelity (Fig. S6†).

Due to the fact that the crosslinking in the produced microgel is not realized by photocrosslinkable methacrylates but *via* the calcium crosslinks, their physico-chemical properties (hydrolytic stability, degradation, mechanical properties, *etc.*, see below) correspond to calcium alginate. For example, the addition of ethylenediaminetetraacetic acid solution to the microgel dispersions resulted in their immediate dissolution due to  $\text{Ca}^{2+}$  decomplexation from the alginate. Also, the degradation properties of the microgels are governed by the calcium decomplexation. We tested the long-term stability of the microgels in aqueous solutions. In neutral  $\text{CaCl}_2$  solution, microgels obtained by basic hydrolysis were stable over the course of at least 3 months without observable changes in their size or morphology (Fig. S7A†). In pure water, some of the microgels preserved their size and shape even after 6 months of storage, while other microgels gradually deformed over the course of several days or weeks (Fig. S7B†). In PBS, the particles swelled and decomposed within several hours as the phosphate anions decomplexed the calcium ions from the crosslinks (Fig. S7C†). Their lability originates from the dynamic nature of the calcium ionic crosslinks and it is characteristic for Ca-alginate microgels. Stabilization methods such as the use of cationic polyelectrolytes<sup>55</sup> can be applied to extend the long-term stability of these materials.

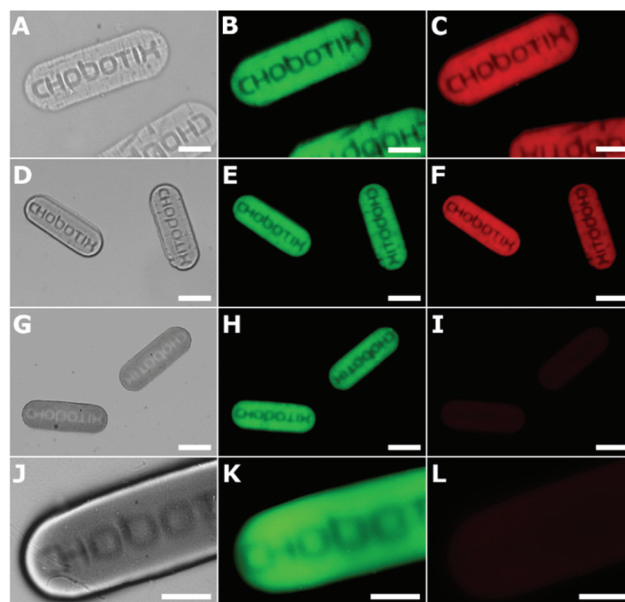
We used a micro-compression test to examine the mechanical properties of the microgels in every stage of lithographic synthesis and postprocessing. Standardly applied methods of the micro-mechanical properties of hydrogels are usually focused on local mechanical properties of the sample, *i.e.* a surface analysis of hydrogel.<sup>56,57</sup> We developed a method to obtain an elastic modulus of the whole sample  $E_s$  (Young's modulus) from the micro-compression test of the whole particle compared to the local mechanical analysis<sup>56,58</sup> (Fig. 3, details can be found in ESI†). The measured elastic modulus of the microgels produced by the SFL without any postprocessing ( $E_s = 16.3 \pm 2.0$  kPa) is attributed solely to the Dex-HEMA network as all the alginate has diffused out from the particle before the measurement started (checked by fluorescence microscopy and also by remeasuring the properties after 1 week storage, obtaining identical result). The Dex-HEMA alginate double network microgels exhibited greater modulus by factor 3.4 ( $E_s = 55.1 \pm 2.9$  kPa), clearly showing the contribution of the alginate network. The alginate microgels (obtained by the basic hydrolysis) exhibited the highest modulus ( $E_s = 74.3 \pm 24.8$  kPa), despite the loss of the Dex-HEMA network. We ascribe this increase to the increase network density in the microgel, caused by its shrinkage and concomitant formation of new ionic crosslinks during the tem-

plate removal process. The modulus of prepared microgels falls between the moduli of control macroscopic samples of 1.25% calcium alginate ( $E_s = 23.0 \pm 5.7$  kPa) and 2.5% calcium alginate ( $E_s = 94.2 \pm 12.7$  kPa). Here, we have confined to a basic description of the purely elastic properties of the microgels while the study on the viscoelastic response of microgels is planned, as thermodynamically consistent mathematical models of elastic and viscoelastic behaviour of hydrogels have already been developed<sup>59,60</sup> and *in silico* tools for modelling viscoelasticity in general branch-on-branch polymer networks are widely available.<sup>61,62</sup>

To demonstrate, that the developed method is not limited to alginate as a substrate, we used it to synthesize **chitosan** microgels. We treated freshly produced Dex-HEMA microgels with entrapped chitosan with genipin – a biocompatible crosslinker widely used for gelation of aminated polysaccharides and proteins in various bioapplications.<sup>39–41</sup> During a 4 hour incubation with genipin, the microgels shrank isotropically from an initial length of  $240 \pm 8 \mu\text{m}$  to  $141 \pm 1 \mu\text{m}$  (41%), indicating the formation of new crosslinks in the network.<sup>45</sup> Simultaneously, the microgels darkened in brightfield microscopy images as a result of the intensive blue colour of the genipin crosslinks.<sup>39–41</sup> The kinetics of the covalent chitosan crosslinking is much slower compared to the ionic alginate crosslinking. The minimal genipin incubation time needed to form a chitosan network that was sufficiently crosslinked to sustain subsequent template removal was 2 hours. Chitosan leakage from the Dex-HEMA crosslinked hydrogel appears to be slow enough for our method to be successful, suggesting that the approach can also be applied to other biopolymers with slow crosslinking kinetics.

After genipin crosslinking, the Dex-HEMA network was basically hydrolyzed in the same manner as in the alginate microgels (Fig. 4). As an alternative to basic hydrolysis, we also successfully exploited dextranase cleavage of the template (Fig. S8†); the microgels obtained by this method were indistinguishable from those obtained *via* basic hydrolysis. After the removal of the Dex-HEMA template, the microgels shrank to  $135 \pm 2 \mu\text{m}$  (by 4% compared to the IPN). The covalently crosslinked chitosan particles were stable long-term in aqueous buffers without any signs of deterioration after several months.

Notably, microgels in both systems studied – chitosan and alginate – shrank significantly during processing with respect to their sizes immediately following lithographic synthesis, while maintaining the features from the lithographic process. While the chitosan microgels shrank dominantly during the first step (IPN formation), the alginate hydrogels shrank dominantly during the second step (template removal). We attribute this difference to the different natures of the biopolymer crosslinks. During IPN formation, the covalent chitosan crosslinks apparently have sufficient binding energies to overcome the elastic energy of the Dex-HEMA network, which results in significant shrinkage of the microgel. This does not occur in the alginate system, as the dynamic ionic crosslinks have much lower binding energies. In the template removal step, the algi-



**Fig. 4** Micrographs of chitosan anisotropic hydrogels. (A) Hydrogels obtained from lithographic synthesis contain non-crosslinked chitosan physically entrapped in the photocrosslinked network of Dex-HEMA. (B and C) Fluorescent images of labelled chitosan and labelled Dex-HEMA, respectively. (D–F) The same sample after treatment with genipin. Samples are shown in brightfield, chitosan fluorescence, and Dex-HEMA fluorescence, respectively. (G–L) Samples after the addition of a base (brightfield – G; chitosan fluorescence – H and K; Dex-HEMA fluorescence – I and L). Scalebar = 50  $\mu\text{m}$  in panels A–I and 25  $\mu\text{m}$  in J–L. All fluorescence images are in false colours.

nate network shrinks likely *via* freshly formed calcium ion bridges as the template is washed away. In contrast, at this stage the chitosan network has already been established and no new crosslinks can be formed (no genipin is present in the solution), so the microgel volume remains constant upon Dex-HEMA hydrolysis.

We also investigated possibilities for ionic crosslinking of chitosan by phytic acid<sup>63</sup> in the process in an analogy to the ionic crosslinking of alginate, followed by enzymatic cleavage of the template (the basic hydrolysis would lead to chitosan deprotonation and hence ionic crosslink destabilization). We were not able to achieve reproducible results, often the microgels lose their shapes during the template removal step (images of successful and unsuccessful results can be found in the Fig. S9†) and further investigation and adjustment of process conditions are needed (chitosan concentration and  $M_w$ , Dex-HEMA methacrylation degree, *etc.*). Despite the low reproducibility of the procedure, we clearly observed shrinking of the ionically crosslinked chitosan microgels during the IPN removal step, similarly to the alginate microgels and contrasting with the covalently crosslinked chitosan. This result supports our above-stated ideas on the origin of shrinking.

The presented method allows production of arbitrarily shaped microgels composed from chemically unmodified biopolymers.

Prepared particles may be used as elemental units for the construction of artificial tissues *via* self-assembly as was previously described with  $\sim 0.5$  mm synthetic polymer blocks prepared by photolithography.<sup>5,64,65</sup> High resolution and high throughput of the SFL combined with the biocompatibility and potential bioactivity of chemically unmodified biopolymers can bring this approach closer towards applications. The variability of crosslinking mechanisms in chemically unmodified polymers enables the manufacture of microgels of variable mechanical properties, that can govern their interaction with living surrounding<sup>66</sup> and, simultaneously, allows for temporal programming of the gels.<sup>34,37</sup>

The presented method also represents a crucial advance with respect to the regulation policy in biomedical applications, the food, and pharmaceutical industries. Regulation mechanisms in these fields are strict and any new synthetic material must undergo a demanding approval process. Our method provides a tool for the microscale shaping of biopolymers, which are already approved in these applications. Alginate is generally recognized as safe material and thus is approved as an additive in the food and pharmaceutical industries.<sup>67</sup> We recently reported a new anticounterfeiting method for food and pharmaceutical products, relying on microscopic hydrogel microtaggants bearing an authenticity code in their topography.<sup>16</sup> New anti-counterfeiting technologies are urgently needed in the pharmaceutical industry due to the alarming rise in counterfeiting rates, reaching 10% of all phar-

maceuticals sold worldwide.<sup>68,69</sup> Producing microtaggants from approved alginate brings the tagging method much closer to a real-life application. Alginate taggants can be used to directly label the surfaces of oral solid formulations (Fig. 5) and can be safely administered together with the formulation.

## Conclusions

We presented a new method to shape biopolymers on a micron-scale. We exploited lithographic processing of a biopolymer mixture with a degradable photocrosslinkable template. Compared to previous lithographic processes with pure biopolymers, our method offers unprecedented resolution and provides a scalable synthesis of anisotropic microgels in sizes ranging from tens to hundreds of micrometres. We plan to further expand the number of biopolymers that can be processed with our method; the only requirement is miscibility with a suitable photocrosslinkable template. This process is also compatible with other photolithographic methods, such as photolithography or stereolithography. Since the resulting (micro)objects are composed solely from a biopolymer, the approval process for their use in biomedical, pharmaceutical or food industry application will be much easier, than of those, composed from synthetic hydrogels.

## Conflicts of interest

There are no conflicts to declare.

## Acknowledgements

We thank Dr Alexandr Zubov for his help with the manuscript. We acknowledge Junior CSF research grant n o. 18-19170Y. I. R. acknowledges his J.E. Purkyne fellowship. The work of P. C. was supported by the European Regional Development Fund; OP RDE; Project: “Chemical biology for drugging undruggable targets (Chem-BioDrug)” (no. CZ.02.1.01/0.0/0.0/16\_019/0000729). The work of J. S. was supported by the Czech Science Foundation, project no. 16-14758S. The work of Y. N. V. K. was supported from the grant of Specific university research – grant No A1\_FCHI\_2020\_005IGA.

## Notes and references

- 1 T. J. Merkel, S. W. Jones, K. P. Herlihy, F. R. Kersey, A. R. Shields, M. Napier, J. C. Luft, H. Wu, W. C. Zamboni, A. Z. Wang, J. E. Bear and J. M. DeSimone, *Proc. Natl. Acad. Sci. U. S. A.*, 2011, **108**, 586–591.
- 2 J. C. Sunshine, K. Perica, J. P. Schneck and J. J. Green, *Biomaterials*, 2014, **35**, 269–277.
- 3 S. Mitragotri, P. A. Burke and R. Langer, *Nat. Rev. Drug Discovery*, 2014, **13**, 655–672.



**Fig. 5** Alginite taggants (manufactured in 2x the nominal size from the Fig. 1) on the surface of oral solid formulation (fluorescence image). Alginate is approved as an additive in the food and pharmaceutical industry which will facilitate the approval process of such taggants. Scalebar corresponds to 50  $\mu\text{m}$ .

- 4 Y. Li, W. Liu, F. Liu, Y. Zeng, S. Zuo, S. Feng, C. Qi, B. Wang, X. Yan, A. Khademhosseini, J. Bai and Y. Du, *Proc. Natl. Acad. Sci. U. S. A.*, 2014, **111**, 13511–13516.
- 5 S. Guven, P. Chen, F. Inci, S. Tasoglu, B. Erkmén and U. Demirci, *Trends Biotechnol.*, 2015, **33**, 269–279.
- 6 A. Khademhosseini and R. Langer, *Biomaterials*, 2007, **28**, 5087–5092.
- 7 M. E. Helgeson, S. C. Chapin and P. S. Doyle, *Curr. Opin. Colloid Interface Sci.*, 2011, **16**, 106–117.
- 8 M. Lunzer, L. Shi, O. G. Andriotis, P. Gruber, M. Markovic, P. J. Thurner, D. Ossipov, R. Liska and A. Ovsianikov, *Angew. Chem., Int. Ed.*, 2018, **57**, 15122–15127.
- 9 J. L. Perry, K. P. Herlihy, M. E. Napier and J. M. DeSimone, *Acc. Chem. Res.*, 2011, **44**, 990–998.
- 10 D. Dendukuri, S. S. Gu, D. C. Pregibon, T. A. Hatton and P. S. Doyle, *Lab Chip*, 2007, **7**, 818–828.
- 11 H. An, H. B. Eral, L. Chen, M. B. Chen and P. Doyle, *Soft Matter*, 2014, **10**, 7595–7605.
- 12 R. Haghgooeie, M. Toner and P. S. Doyle, *Macromol. Rapid Commun.*, 2010, **31**, 128–134.
- 13 Y. Du, E. Lo, S. Ali and A. Khademhosseini, *Proc. Natl. Acad. Sci. U. S. A.*, 2008, **105**, 9522–9527.
- 14 P. Panda, S. Ali, E. Lo, B. G. Chung, T. A. Hatton, A. Khademhosseini and P. S. Doyle, *Lab Chip*, 2008, **8**, 1056.
- 15 D. K. Hwang, J. Oakey, M. Toner, J. A. Arthur, K. S. Anseth, S. Lee, A. Zeiger, K. J. Van Vliet and P. S. Doyle, *J. Am. Chem. Soc.*, 2009, **131**, 4499–4504.
- 16 I. Rehor, S. van Vreeswijk, T. Vermonden, W. E. Hennink, W. K. Kegels and H. B. Eral, *Small*, 2017, **13**, 1701804.
- 17 S. M. Mihaila, A. K. Gaharwar, R. L. Reis, A. P. Marques, M. E. Gomes and A. Khademhosseini, *Adv. Healthcare Mater.*, 2013, **2**, 895–907.
- 18 K. Yue, G. Trujillo-de Santiago, M. M. Alvarez, A. Tamayol, N. Annabi and A. Khademhosseini, *Biomaterials*, 2015, **73**, 254–271.
- 19 A. O. Elzoghby, W. M. Samy and N. A. Elgindy, *J. Controlled Release*, 2012, **161**, 38–49.
- 20 A. Drucker and M. Pratt, *Dermatitis*, 2011, **22**, 98–101.
- 21 K. Aalto-Korte, K. Alanko, O. Kuuliala and R. Jolanki, *Contact Dermatitis*, 2007, **57**, 324–330.
- 22 K. Aalto-Korte, M.-L. Henriks-Eckerman, O. Kuuliala and R. Jolanki, *Contact Dermatitis*, 2010, **63**, 301–312.
- 23 L. Giroux and M. D. Pratt, *Am. J. Contact Dermatitis*, 2002, **13**, 143–145.
- 24 M. A. Lemp, *Curr. Opin. Allergy Clin. Immunol.*, 2008, **8**, 457.
- 25 A. Spencer, P. Gazzani and D. A. Thompson, *Contact Dermatitis*, 2016, **75**, 157–164.
- 26 N. Goonoo, A. Bhaw-Luximon, G. L. Bowlin and D. Jhurry, *Polym. Int.*, 2013, **62**, 523–533.
- 27 J. K. Oh, D. I. Lee and J. M. Park, *Prog. Polym. Sci.*, 2009, **34**, 1261–1282.
- 28 S. K. Nitta and K. Numata, *Int. J. Mol. Sci.*, 2013, **14**, 1629–1654.
- 29 S. Grijalvo, J. Mayr, R. Eritja and D. D. Díaz, *Biomater. Sci.*, 2016, **4**, 555–574.
- 30 T. T. Dang, Q. Xu, K. M. Bratlie, E. S. O'Sullivan, X. Y. Chen, R. Langer and D. G. Anderson, *Biomaterials*, 2009, **30**, 6896–6902.
- 31 C. Qiu, M. Chen, H. Yan and H. Wu, *Adv. Mater.*, 2007, **19**, 1603–1607.
- 32 G. Talei Franzesi, B. Ni, Y. Ling and A. Khademhosseini, *J. Am. Chem. Soc.*, 2006, **128**, 15064–15065.
- 33 A. I. Neto, K. Demir, A. A. Popova, M. B. Oliveira, J. F. Mano and P. A. Levkin, *Adv. Mater.*, 2016, **28**, 7613–7619.
- 34 Y. Fumiki, K. Hirokazu, J. Yun-Ho, B. Hojae, Y. Du, F. Junji, Qi Hao and K. Ali, *J. Biomed. Mater. Res., Part A*, 2011, **97**, 93–102.
- 35 V. Javvaji, A. G. Baradwaj, G. F. Payne and S. R. Raghavan, *Langmuir*, 2011, **27**, 12591–12596.
- 36 B. Chueh, Y. Zheng, Y. Torisawa, A. Y. Hsiao, C. Ge, S. Hsiong, N. Huebsch, R. Franceschi, D. J. Mooney and S. Takayama, *Biomed. Microdevices*, 2010, **12**, 145–151.
- 37 T. M. Valentin, S. E. Leggett, P.-Y. Chen, J. K. Sodhi, L. H. Stephens, H. D. McClintock, J. Y. Sim and I. Y. Wong, *Lab Chip*, 2017, **17**, 3474–3488.
- 38 Z. Liu, M. Takeuchi, M. Nakajima, C. Hu, Y. Hasegawa, Q. Huang and T. Fukuda, *Acta Biomater.*, 2017, **50**, 178–187.
- 39 P. Somers, F. De Somer, M. Cornelissen, S. Bouchez, F. Gasthuys, K. Narine, E. Cox and G. Van Nooten, *J. Heart Valve Dis.*, 2008, **17**, 682.
- 40 M. F. Butler, Y.-F. Ng and P. D. A. Pudney, *J. Polym. Sci., Part A: Polym. Chem.*, 2003, **41**, 3941–3953.
- 41 R. A. A. Muzzarelli, *Carbohydr. Polym.*, 2009, **77**, 1–9.
- 42 W. N. E. van Dijk-Wolthuis, S. K. Y. Tsang, J. J. Kettenes-van and den Bosch, W. E. Hennink, *Polymer*, 1997, **38**, 6235–6242.
- 43 B. D. Fairbanks, M. P. Schwartz, C. N. Bowman and K. S. Anseth, *Biomaterials*, 2009, **30**, 6702–6707.
- 44 W. N. E. van Dijk-Wolthuis, J. A. M. Hoogboom, M. J. Van Steenbergen, S. K. Y. Tsang and W. E. Hennink, *Macromolecules*, 1997, **30**, 4639–4645.
- 45 T. Canal and N. A. Peppas, *J. Biomed. Mater. Res.*, 1989, **23**, 1183–1193.
- 46 L. Pescosolido, T. Vermonden, J. Malda, R. Censi, W. J. A. Dhert, F. Alhaique, W. E. Hennink and P. Matricardi, *Acta Biomater.*, 2011, **7**, 1627–1633.
- 47 P. Matricardi, M. Pontoriero, T. Coviello, M. A. Casadei and F. Alhaique, *Biomacromolecules*, 2008, **9**, 2014–2020.
- 48 H. Li, *Smart Hydrogel Modelling*, Springer Science & Business Media, 2010.
- 49 P. O. Baburkin, P. V. Komarov, S. D. Khizhnyak and P. M. Pakhomov, *Colloid J.*, 2015, **77**, 561–570.
- 50 D. V. Guseva, V. Y. Rudyak, P. V. Komarov, A. V. Sulimov, B. A. Bulgakov and A. V. Chertovich, *J. Polym. Sci., Part B: Polym. Phys.*, 2018, **56**, 362–374.
- 51 A. Hajikhani, F. Scocozza, M. Conti, M. Marino, F. Auricchio and P. Wriggers, *Int. J. Artif. Organs*, 2019, **42**, 548–557.

- 52 P. J. Flory, *Principles of Polymer Chemistry*, Cornell University Press, 1953.
- 53 C. M. Hansen, *Hansen Solubility Parameters: A User's Handbook*, CRC Press, 2002.
- 54 S. Mytnyk, A. G. L. Olive, F. Versluis, J. M. Poolman, E. Mendes, R. Eelkema and J. H. van Esch, *Angew. Chem., Int. Ed.*, 2017, **56**, 14923–14927.
- 55 Z. Li, H. R. Ramay, K. D. Hauch, D. Xiao and M. Zhang, *Biomaterials*, 2005, **26**, 3919–3928.
- 56 A. M. Padoł, K. I. Draget and B. T. Stokke, *Carbohydr. Polym.*, 2016, **147**, 234–242.
- 57 C. A. Verheyen, L. Morales, J. Sussman, K. Paunovska, V. Manzoli, N. M. Ziebarth and A. A. Tomei, *Macromol. Mater. Eng.*, 2019, **304**, 1800679.
- 58 K. L. Johnson and K. L. Johnson, *Contact Mechanics*, Cambridge University Press, 1987.
- 59 D. Caccavo, A. Vietri, G. Lamberti, A. A. Barba and A. Larsson, in *Computer Aided Chemical Engineering*, ed. D. Manca, Elsevier, 2018, vol. 42, pp. 357–383.
- 60 D. Caccavo, S. Cascone, G. Lamberti and A. A. Barba, *Chem. Soc. Rev.*, 2018, **47**, 2357–2373.
- 61 C. Das, W. Li, D. J. Read and J. M. Soulages, *Rheol. Acta*, 2019, **58**, 159–172.
- 62 A. Zubov and G. Sin, *Chem. Eng. J.*, 2018, **336**, 361–375.
- 63 H. Lee, C. Jeong, K. Ghafoor, S. Cho and J. Park, *Bio-Med. Mater. Eng.*, 2011, **21**, 25–36.
- 64 G. Fernandez Javier and Khademhosseini Ali, *Adv. Mater.*, 2010, **22**, 2538–2541.
- 65 H. Qi, M. Ghodousi, Y. Du, C. Grun, H. Bae, P. Yin and A. Khademhosseini, *Nat. Commun.*, 2014, **4**, 2275.
- 66 P. Guo, D. Liu, K. Subramanyam, B. Wang, J. Yang, J. Huang, D. T. Auguste and M. A. Moses, *Nat. Commun.*, 2018, **9**, 130.
- 67 *Direct Food Substances Affirmed as Generally Recognized as Safe*.
- 68 WHO | Substandard, spurious, falsely labelled, falsified and counterfeit (SSFFC) medical products, <http://www.who.int/mediacentre/factsheets/fs275/en/>, (accessed June 28, 2016).
- 69 Background Information – FIP – International Pharmaceutical Federation Counterfeit medicines, [http://www.fip.org/www/index.php?page=menu\\_counterfeitmedicines\\_policy](http://www.fip.org/www/index.php?page=menu_counterfeitmedicines_policy), (accessed July 1, 2016).